

Thermodynamics and Phase Diagram of High Temperature Superconductors

Philippe Curty and Hans Beck

Université de Neuchâtel, 2000 Neuchâtel, Switzerland
(Received 7 August 2002; published 15 December 2003)

Thermodynamic quantities are derived for superconducting and pseudogap regimes by taking into account both amplitude and phase fluctuations of the pairing field. In the normal (pseudogap) state of the underdoped cuprates, two domains have to be distinguished: near the superconducting region, phase correlations are important up to temperature T_ϕ . Above T_ϕ , the pseudogap region is determined only by amplitudes, and phases are uncorrelated. Our calculations show excellent quantitative agreement with specific heat and magnetic susceptibility experiments on cuprates. We find that the mean field temperature T_0 has a similar doping dependence as the pseudogap temperature T^* , whereas the pseudogap energy scale is given by the average amplitude above T_c .

DOI: 10.1103/PhysRevLett.91.257002

PACS numbers: x74.72.-h, 71.10.Fd, 74.20.Mn, 74.40.+k

One of the most intriguing problems in high temperature superconductivity is the presence of a region above the critical temperature T_c and below a temperature T^* where observable quantities deviate from Fermi liquid behavior. This region is called the pseudogap region [1,2] because it contains effects similar to superconductivity such as a partial suppression of electronic density of states.

The origin of such a pseudogap above T_c is unclear. There are four major approaches concerning its theoretical understanding: the first is based on the formation of incoherent Cooper pairs above T_c . Phase order [3] or Bose condensation [4] would then establish superconductivity at T_c . The second assumes that the pseudogap is induced by antiferromagnetic fluctuations [5]. The third approach is based on spin-charge separation where spins bind together to form spin singlets and the energy needed to split them apart leads to the formation of a "spin gap" [6]. The fourth assumes the existence of a quantum critical point [7] but the latter has never been observed. However, these approaches seem to be unable to describe specific heat and magnetic susceptibility.

The main aim of this Letter is to show that various experimental observations can indeed be interpreted in terms of fluctuations of the pairing field $\psi = |\psi|e^{i\phi}$ and that two temperature regions have to be distinguished (see Fig. 5): for a relatively small temperature interval $T_c < T < T_\phi$ the phase of ψ is still uncorrelated in space over some correlation length ξ (the Kosterlitz-Thouless correlation length in 2D). Thus, in this regime, observables are governed by correlated phase fluctuations described by the XY model. For $T_\phi < T < T^*$, phases of ψ are essentially uncorrelated (ξ is on the order of the lattice constant), but $|\psi|$ is still fluctuating and nonzero, signaling local pair fluctuations. This explains the wide hump seen in specific heat experiments [1], the depression of the spin susceptibility [8], and the persistence of the pseudogap for $T < T^*$.

Our method has a major difference with respect to the Emery and Kivelson phase fluctuations scenario [3] of the pseudogap regime: we show that phase fluctuations influence the pseudogap only up to a temperature T_ϕ , which is much smaller than T^* . Above T_ϕ , observables are thus determined only by the amplitude of the pairing field.

The picture of two different regimes above T_c is also supported by other experiments: (a) Demsar *et al.* [9], interpreting the real-time measurements of the quasiparticle relaxation dynamics, find a temperature interval of only a few K in which pair fluctuations associated with their collective phase are important, whereas the pseudogap persists to much higher temperatures. (b) Hall effect measurements [10] in underdoped GdBa₂Cu₃O_{7-x} show a characteristic temperature T' between T_c and T^* , at which the temperature dependence of $\cot(\Theta_H)$ deviates from T^2 and the Hall coefficient has a peak. A possible explanation consists in considering vortex excitations as scattering centers modifying the Hall angle Θ_H and Hall coefficient, which would again suggest identifying T' with our T_ϕ , below which correlated vortices exist.

We base our calculations on a d -wave attractive Hubbard model

$$H = -t \sum_{\langle i,j \rangle \sigma} c_{i\sigma}^\dagger c_{j\sigma} - U \sum_i Q_d^\dagger(i) Q_d(i), \quad (1)$$

with a hopping t between nearest neighbor sites i and j on a square lattice. The interaction favors the formation of onsite d -wave pairs since $Q_d^\dagger(i) = \sum_j D_{ij} Q_{ij}^\dagger$, where $D_{ij} = 1, (-1)$ for i being the nearest neighbor site of j in the horizontal (vertical) direction. $Q_{ij}^\dagger = (c_{i\uparrow}^\dagger c_{j\downarrow}^\dagger - c_{i\downarrow}^\dagger c_{j\uparrow}^\dagger) / \sqrt{2}$ is the singlet pair operator of neighboring sites. Decoupling the interaction with the help of a Stratonovich-Hubbard transformation, the partition function $Z = \text{Tr} e^{-\beta H}$ is then

$$Z = Z_n \int D^2 \psi \langle \mathcal{T} e^{-\int_0^\beta d\tau \sum_i (1/U |\psi|^2 + \psi Q_d^\dagger(i) + \text{H.c.})} \rangle_{H_n},$$

where $\psi = \psi(i, \tau) = |\psi(i, \tau)|e^{i\phi(i, \tau)}$, and H_n is the non-interacting part. The trace over the fermionic operators can be evaluated, yielding

$$Z = \int D^2\psi e^{-\int_0^\beta d\tau [\sum_r 1/U|\psi|^2 + \text{Tr} \ln G]} \quad (2)$$

Here G is a Nambu matrix of one-electron Green functions for fermions interacting with a given space and time dependent pairing field $\psi(i, \tau)$.

Expanding (2) in powers of $\vec{\nabla}\psi$, Z can be written as a functional integral involving an action $S[\psi]$ for a field ψ that changes slowly in space and that can be taken time independent:

$$S[\psi] = \int d^d r [S_0(|\psi|) + S_1(\vec{\nabla}\psi)], \quad (3)$$

where S_0 is a local function of $|\psi(\mathbf{r})|$, and $S_1 = c|\vec{\nabla}\psi|^2/2$ where c is a constant. d is the dimension.

Now we compute observables such as energy, specific heat, and spin susceptibility. Our main strategy is to treat separately amplitude and phase fluctuations. In this spirit, two different approaches are possible: (i) The amplitude is fixed and determined by a suitable variational equation. (ii) The energy is expanded around the average amplitude.

Variational method.—We can neglect amplitude correlations since simulations show that they are weak between different sites i, j : $\langle |\psi_i| |\psi_j| \rangle - \langle |\psi|^2 \rangle \approx 0$ (i.e., the amplitude is always positive and shows no critical behavior). Rewriting the free energy F in terms of a constant amplitude $|\bar{\psi}|$ yields

$$F = -\frac{1}{\beta} \log \int D\phi e^{-\beta[V S_0(|\bar{\psi}|)V/\beta + \int d^d r S_1]},$$

where the Jacobian of the polar transformation is put into the exponential, and V is the volume. Equating the derivative of F with respect to $|\bar{\psi}|$ to zero leads to the self-consistent equation:

$$\frac{\partial S_0(|\bar{\psi}|)}{\partial |\bar{\psi}|} - \frac{1}{\beta |\bar{\psi}|} + c|\bar{\psi}| \langle |\vec{\nabla} e^{i\phi}|^2 \rangle_{XY} = 0. \quad (4)$$

The first term, called the amplitude contribution, leads to the BCS gap equation [11] if other contributions are neglected. The second comes from the Jacobian and implies that the amplitude is never zero. The third term is the expectation value of the energy in the XY model depending on the constant coupling $c|\bar{\psi}|^2/2$. This contribution characterizes the influence of the phase fluctuations. Solutions of Eq. (4) are reliable for all temperatures except for $T \ll T_c$. They are accurate at T_c only in the underdoped regime.

Average value method.—Now we keep the local coupling in S_1 between amplitude and phase by introducing the statistical Ginzburg-Landau (GL) model (see Ref. [12]). Averages such as $\langle |\psi| \rangle$ and $\langle S_1 \rangle$ are computed within the GL model with all fluctuations and correla-

tions. Then fermionic observables are expanded with respect to the average amplitude.

Expanding the energy density obtained from action (3) around the average amplitude (see Fig. 1) yields

$$E = \langle S \rangle_S / V \approx S_0(\langle |\psi| \rangle) + \langle S_1 \rangle_S + \mathcal{O}(\langle \delta |\psi|^2 \rangle), \quad (5)$$

where the square of amplitude fluctuations is neglected in the first approximation. Averages are computed using a normalized GL action:

$$S_{\text{GL}}[\psi] = k_B V_0 \int d^d r (U_{\text{GL}} + |\vec{\nabla}\psi|^2/2), \quad (6)$$

where $U_{\text{GL}} = \eta^2[(T/T_0 - 1)|\tilde{\psi}(\mathbf{r})|^2 + |\tilde{\psi}(\mathbf{r})|^4/2]$ comes from the expansion of S_0 in powers $\beta|\psi|$. T_0 is the mean field pairing temperature, and $\tilde{\psi} = \psi/|\psi_0|$, where $\psi_0 = \psi(T=0)$. S_{GL} is normalized with a lattice spacing ε . $\eta := \varepsilon/\xi_0$, where ξ_0 is the mean field correlation length at zero temperature. V_0 is the zero temperature phase stiffness. The energy becomes

$$E \approx S_0(\langle |\psi| \rangle_{\text{GL}}) + \langle S_1 \rangle_{\text{GL}}, \quad (7)$$

where $S_0(\langle |\psi| \rangle) = (\langle |\psi|^2 \rangle / U) - \frac{2}{\beta V} \sum_q \log[2 \cosh \beta E_q / 2]$ corresponds the BCS free energy for which the gap value is determined by the GL average. The d -wave quasiparticle energy is $E_q = [(\varepsilon_q - \mu)^2 + \langle |\psi|^2 \rangle \cos^2(2\theta)]^{1/2}$, where μ is the chemical potential and θ is the angle in k space with respect to the k_x direction.

For computer simulations of the statistical ensemble $\{\psi\}$ under the action S_{GL} , we use a standard Monte Carlo procedure to update amplitude $|\tilde{\psi}|$ and a Wolff [13] algorithm for the phase ϕ as for the real Φ^4 model [14]. Typically, 10^4 sweeps are needed to obtain good statistics for lattice size: $N = 40^2$. The value of η modifies slightly the shape of the average amplitude. The link between S_0 and the GL action is made by fixing the ratio of $|\psi_0|$ and T_0 . Since we are interested in the temperature domain from T_c to T^* , the ratio $|\psi_0|/T_0$ is fixed at $T = T_c$

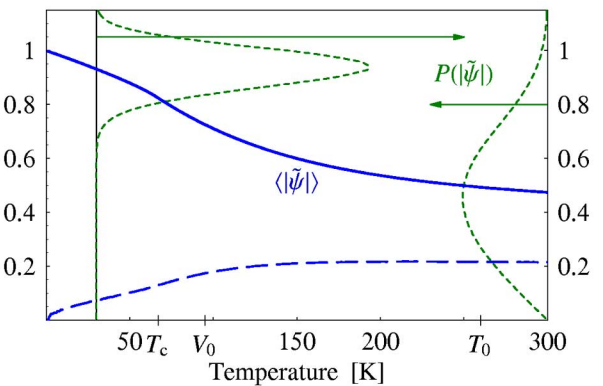


FIG. 1 (color online). Average amplitude $\langle |\tilde{\psi}| \rangle$ (thick line) and the corresponding standard deviation $(\langle |\tilde{\psi}|^2 \rangle - \langle |\tilde{\psi}| \rangle^2)^{1/2}$ (long-dashed line) from 2D GL simulations. Parameters are $V_0 = 95$ K, $T_0 = 260$ K. Dashed curves: amplitude distribution $P(|\tilde{\psi}|)$ (histogram) for $T = 300$ K (right) and $T = 30$ K (left).

by requiring that the specific heat jump recovers its BCS value in the overdoped regime. We found that this ratio must be $|\psi_0|/T_0 = 3.06$ in the s -wave case, and $|\psi_0|/T_0 = 3.72$ for d -wave symmetry.

Both approaches are valid below and above the critical temperature T_c , which is the temperature where the phase stiffness becomes zero.

The specific heat C is the sum of C_0 and C_1 , amplitude and gradient contributions, respectively. Defining $\gamma = C/(\gamma_n T)$ where γ_n is the Sommerfeld constant, the reduced specific heat is

$$\gamma = \gamma_0(\langle|\psi|\rangle) + \gamma_1, \quad (8)$$

where γ_1 is divided by T_c instead of T since S_1 is classical and does not satisfy the third law of thermodynamics.

The amplitude contribution γ_0 is 1 at high temperature. The gradient contribution is normalized as:

$$\frac{C_1}{\gamma_n} = \frac{k_B}{\xi_0^3 \gamma_n} \frac{C_1^{(s)}}{Nk_B}, \quad (9)$$

where $V = N\xi_0^3$, and $C_1^{(s)}/(Nk_B)$ is the specific heat per number of lattice sites coming from the simulations. Experiments give $\gamma_n \approx 26 \text{ mJ K}^{-1} \text{ mol}^{-1} = 252 \text{ J K}^{-1} \text{ m}^{-3}$. For the fit of Fig. 2, using the reasonable value $\xi_0 \approx 16 \text{ \AA}$, we get the dimensionless constant $\alpha = k_B/(\xi_0^3 \gamma_n) \approx 13.5$. In Fig. 2 the experimental specific heat of $\text{YBa}_2\text{Cu}_3\text{O}_{6.73}$ [1] is fitted using the variational method reproducing the double peak structure: a sharp peak at T_c coming mainly from correlated phase fluctuations and a wide hump rounded by amplitude fluctuations (see Fig. 1 for typical distributions). The crossover temperature T_1 corresponds to the temperature where γ_1 is less than approximately 2% of the normal specific heat. In the amplitude equation (4), a two-dimensional density of states $D(\varepsilon) = 1/W$ is used with $W = 5000 \text{ K}$, $\mu = 0.25W$, and $U = 959 \text{ K}$. These values give $T_0 \approx 200 \text{ K}$

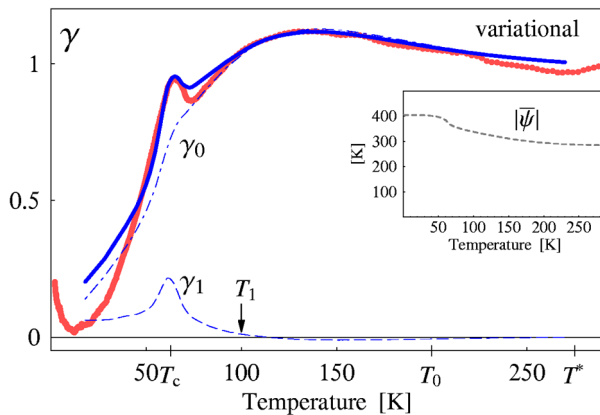


FIG. 2 (color online). The specific heat from the variational method (thick line), which is the sum of gradient (dashed line) and amplitude (dot-dashed line) contributions, reproduces measurements of $\text{YBa}_2\text{Cu}_3\text{O}_{6.73}$ (points). Inset: T dependent amplitude $|\psi|$ from Eq. (4).

257002-3

and $\psi_0 \approx 2.14T_0$ in agreement with experiments [15]. The other parameters are $V_0 = 72 \text{ K}$ and $\eta = 5$.

The average value method is used to reproduce specific heat measured for different dopings in Fig. 3. For underdoped systems $x < 0.80$ we use simulations in $d = 2$. For the more overdoped, $x \geq 0.80$, simulations are done in $d = 3$. Parameters V_0 and T_0 extracted from the best fits are shown in the phase diagram of Fig. 5. α ranges from 7 to 15.

The magnetic susceptibility χ has two contributions: the paramagnetic spin susceptibility χ_p and the orbital diamagnetic susceptibility χ_d . χ_p has been measured by Takigawa *et al.* [8] on powder $\text{YBa}_2\text{Cu}_3\text{O}_{6.63}$ using Cu and O NMR experiments. The direct contribution coming from phases is negligible because NMR probes essentially the presence of pairs which is related to the amplitude. Therefore, χ_p is given by the amplitude contribution:

$$\chi_p = \frac{\chi_0}{2T} \int_0^{2\pi} \frac{d\theta}{2\pi} \int_0^\infty d\varepsilon \cosh^{-2} \sqrt{\frac{\varepsilon^2 + \langle|\psi|\rangle_{\text{GL}}^2 \cos^2(2\theta)}{2T}}. \quad (10)$$

χ_0 is the Pauli spin susceptibility. In Fig. 4, we compare the result of Eq. (10) and Takigawa's measurements on powder $\text{YBa}_2\text{Cu}_3\text{O}_{6.63}$. The best fit yields $T_0 = 159.2 \text{ K}$, $V_0 = 59.3 \text{ K}$. The competition between amplitude and thermal energy enters into the spin susceptibility (10) by the ratio $\langle|\psi|\rangle/T$. The temperature T_ϕ where phases start to influence the thermodynamics is the temperature where $\langle|\psi|\rangle$ deviates from the average amplitude computed for random phases. This temperature is found above T_c at $T_\phi \approx 90 \text{ K}$. The orbital diamagnetic susceptibility χ_d in $\text{YBa}_2\text{Cu}_3\text{O}_{6.60}$ shows fluctuation effects up to about 15 K above T_c . For $T > T_\phi$, phase fluctuations are so strong that χ_d vanishes [16].

The Green function can be calculated in coherent potential approximation (CPA) for electrons that are scattered from spatially uncorrelated "pair impurities." We extended the s -wave CPA [17] by using a d -wave amplitude and uncorrelated phases. We have computed the

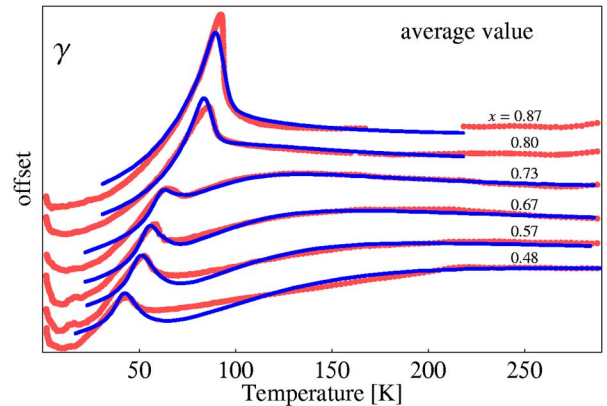


FIG. 3 (color online). Experimental specific heat (points) for $\text{YBa}_2\text{Cu}_3\text{O}_{6+x}$ compared to the average value method.

257002-3

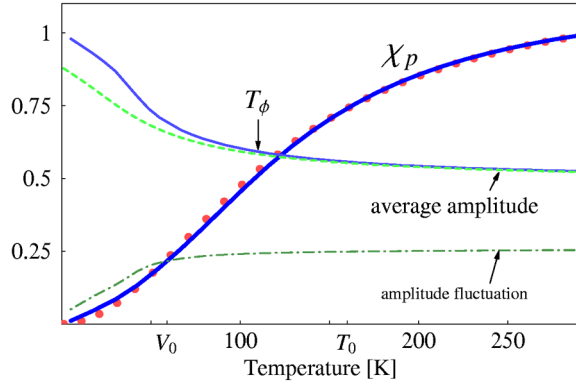


FIG. 4 (color online). The measured spin susceptibility of $\text{YBa}_2\text{Cu}_3\text{O}_{6.63}$ (points) divided by χ_0 is well fitted by the theoretical (thick line) susceptibility χ_p . The dot-dashed line is the standard deviation of the average amplitude.

density of states at half-filling $\mu = 0.5W$ and maximum amplitude $|\psi| = 0.8W$. The result is a pseudogap of width $\Delta \approx 0.2W$, although phases are completely uncorrelated.

Phase diagram.—Values of T_0 , V_0 , and T_ϕ extracted from specific heat fits (Fig. 3) are reported in Fig. 5. T_1 is the temperature where $C_1/\gamma_n = 2\%$. T_ϕ is computed in the same way as shown in Fig. 4 using average amplitudes from specific heat fits. Here it is the temperature where the amplitude differs by 2% from the amplitude in a random phase field. The energy scale $E_g := \langle |\psi| \rangle_{T=200\text{ K}}$ of the pseudogap is defined as the amplitude at $T = 200\text{ K}$. E_g shows the same doping dependence as the one found by Tallon and Loram [18]. However, it is not related to any hidden critical point. Phase correlations above T_c grow rapidly in the underdoped regime following the T_ϕ line and have a similar doping dependence as Nernst effect results [19]. The gradient specific heat from S_1 disappears more rapidly such as in the Hall effect [10].

Discussion.—Amplitude and phase fluctuations are the key for understanding the pseudogap regime of underdoped high temperature superconductors. Phase correlations disappear completely near a temperature T_ϕ above T_c , and therefore, for $T > T_\phi$, the pseudogap region is dominated by amplitude fluctuations. The mean field temperature T_0 has a similar doping dependence as T^* , signaling that the pseudogap region is due to independent fluctuating pairs. Comparisons with measured specific heat on underdoped YBCO reproduce the double peak structure: a sharp peak at T_c coming mainly from phase correlations and a separate wide hump below T^* rounded by fluctuations. The spin susceptibility, related to the amplitude, recovers its normal behavior near T^* , whereas the orbital magnetic susceptibility, related to phases, disappears near T_ϕ . These considerations are independent from the underlying pairing mechanism, and any microscopic theory inducing pairing should lead to similar conclusions.

All of these findings provide additional evidence for the fact that superconductivity and pseudogap have the

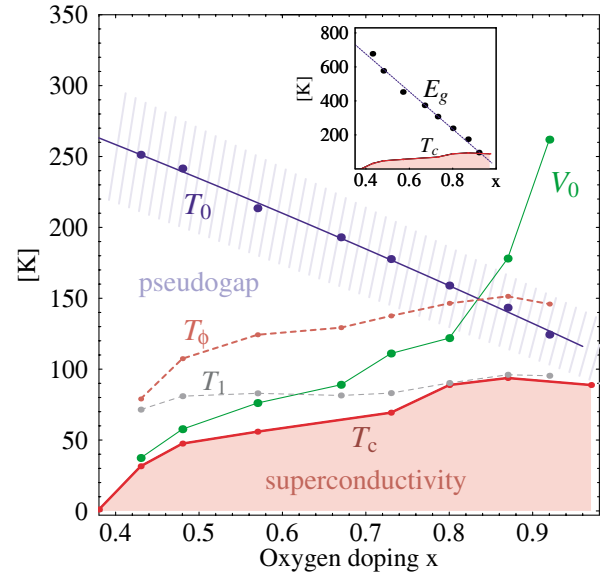


FIG. 5 (color online). Phase diagram of $\text{YBa}_2\text{Cu}_3\text{O}_{6+x}$. Effects of amplitudes are large in the quasi-uncorrelated pseudogap region (below T_0), whereas phase correlations remain important only below T_ϕ . The temperature T^* , where γ and χ_d cross over to normal behavior, is located in the hatched area. Inset: the pseudogap energy scale E_g .

same origin. The former is primarily related to phases of the pairing field, which are ordered below the transition temperature and whose correlations survive over a limited temperature region above T_c . The pseudogap regime of underdoped materials then extends to much higher temperatures due to the persisting amplitude fluctuations of the pairing field.

We thank J. Loram, B. Janko, C. Moca, and C. Wirth. This work has been supported by the Swiss National Science Foundation.

- [1] J.W. Loram *et al.*, Phys. Rev. Lett. **71**, 1740 (1993).
- [2] T. Timusk and S. Bryan, Rep. Prog. Phys. **62**, 61 (1999).
- [3] V.J. Emery and S.A. Kivelson, Nature (London) **374**, 434 (1995).
- [4] M. Randeria and J.C. Campuzano, cond-mat/9709107.
- [5] J. Schmalian *et al.*, Phys. Rev. Lett. **80**, 3839 (1998).
- [6] P.A. Lee, Physica (Amsterdam) **317C–318C**, 194 (1999).
- [7] S. Sachdev, Phys. World **12**, 33 (1999).
- [8] M. Takigawa *et al.*, Phys. Rev. B **43**, 247 (1991).
- [9] J. Demsar *et al.*, Phys. Rev. Lett. **82**, 4918 (1999).
- [10] D. Matthey *et al.*, Phys. Rev. B **64**, 024513 (2001).
- [11] J. Bardeen *et al.*, Phys. Rev. **108**, 1175 (1957).
- [12] Ph. Curty and H. Beck, Phys. Rev. Lett. **85**, 796 (2000).
- [13] U. Wolff, Phys. Rev. Lett. **62**, 361 (1989).
- [14] R.C. Brower *et al.*, Phys. Rev. Lett. **62**, 1087 (1989).
- [15] M. Kugler *et al.*, Phys. Rev. Lett. **86**, 4911 (2001).
- [16] A. Sewer and H. Beck, Phys. Rev. B **64**, 014510 (2001).
- [17] B.L. Gyorffy *et al.*, Phys. Rev. B **44**, 5190 (1991).
- [18] J.L. Tallon and J.W. Loram, cond-mat/0005063.
- [19] Y. Wang *et al.*, Phys. Rev. B **64**, 224519 (2001).